Impact of chamber back pressure on the ignition dynamics of hydrogen enriched premixed flames

Tarik Yahou, James R Dawson, Thierry Schuller

Impact of chamber back pressure on the ignition dynamics of hydrogen enriched premixed flames

Tarik Yahou[a,b,*], James R. Dawson[a], Thierry Schuller[b]

[a] *Department of Energy and Process Engineering, Norwegian University of Science and Technology, Trondheim N-7491, Norway.*
[b] *Institut de Mécanique des Fluides de Toulouse, IMFT, Université de Toulouse, CNRS, Toulouse, France.*

Abstract

The impact of chamber back pressure and H_2-enrichment on flashback of premixed CH_4-H_2-Air flames triggered by ignition dynamics is investigated. Different back pressures are imposed by varying the exhaust flow blockage with perforated plates of different porosities. Experiments measuring the ignition transient, from kernel formation to stable flames and flashback, with increasing levels of H_2-enrichment covering a wide range of operating conditions are conducted. Time-series of pressure, velocity and heat release rate are examined to characterise the ignition process. It is shown that the final state of the flame is highly modified by the over pressure caused by the volumetric expansion of the hot gases. Three different scenarios are identified: Soft ignition with direct stabilisation, transient flashback and permanent flashback. The magnitude of the over pressure generated at ignition is significantly amplified by small increases in mean back pressure which, in turn, modifies the flowrate through the injector thereby promoting flashback. In addition to its role as a pressure amplifier, increasing the combustor back pressure also affects the time lag between the over pressure and the peak in heat release rate just after ignition. The impact of H_2-enrichment on flashback is investigated by keeping both the bulk injection velocity U_b and laminar burning velocity S_l^0 constant for flames with 0% to 100% H_2-content. It is shown that the magnitude of the over pressure approximately scales with U_b/S_l^0 and is independent of the total thermal power and H_2 enrichment. Although the mean flow conditions and over pressures are kept constant, the stabilisation mode directly depends on H_2-content. This shows that flashback triggered by the ignition dynamics cannot be fully described by classical kinematic arguments and a new mechanism is presented.

Keywords: Spark ignition; Flashback mechanism; Combustion dynamics; Hydrogen flames.

1. Introduction

Given the urgent need to substantially cut CO_2 emissions in the face of increasing demand for large-scale power generation, the development of carbon-free technologies is essential. Hydrogen fueled gas turbines are ideally placed to play a major role in accelerating the energy transition towards zero-emission power [1]. However, the higher flammability, flame speed, and diffusivity of hydrogen and hydrogen-enriched mixtures introduces new challenges that must be addressed [2].

In this context, ignition dynamics and flashback raise many issues that need to be considered at the design stage of the engine. For instance, ignition generates an over pressure which can promote flashback inside the injector causing the flame to stabilise in unwanted locations leading to a localised increase in the temperature inside the premixer. Ignition and flashback are phenomena usually studied separately, but the over pressure generated at ignition can lead to flashback.

Spark ignition dynamics have been extensively studied and the process can be categorised into three main steps: i) flame kernel creation, ii) propagation and stabilisation and iii) burner-to-burner flame propagation for multi-injector systems. The fundamental processes underpinning i) and ii) are well documented in terms of spark characteristics, fuel composition and flow velocity [3, 4]. Only recently has research been dedicated to iii), where a large set of data on the light-round process in multi-burner combustors is now available [5, 6]. In single burners, high speed flame visualisations have shown that successful ignition is associated with kernal formation followed by advection and/or propagation to regions close to the anchoring point in order to fully stabilise the combustion reaction. The direction of the instantaneous velocity in the vicinity of the spark has also been shown to play an important role for successful flame growth [7]. Recent direct numerical simulations of ignition in high-speed flows above a backward step combustor [8] have shown that the ability of a flame to propagate into different regions of the flow is essentially controlled by the strain rate in shear regions which can quench the flame and prevent stabilisation.

Compared to constant pressure steady flow combustion systems like gas turbines, a number of investigations on the impact of hydrogen enrichment on the ignition dynamics have been carried out in constant volume chamber or internal combustion engines. Correlations between hydrogen enrichment, the combustion time and the pressure impulse generated at ignition have been established [9]. For example, it has been shown that even at very low levels of hydrogen concentration (2 Vol.$\%$), the combustion time of hydrogen enriched diesel is significantly reduced without any significant changes in the peak cylinder pressure [10]. Conversely, the effect of hydrogen enrichment has been found to be more pronounced for lean combustible mixtures. In [11] it was demonstrated that replacing methane with 15 Vol.$\%$ of hydrogen led to an increase of the pressure peak by an order of magnitude compared to operating with pure methane. However, it is currently unclear what impact H_2 enrichment will have on the ignition dynamics of flames in constant pressure systems.

Furthermore, the interaction between ignition and flashback is not well understood as it has yet to be studied over a wide range of operating conditions and geometries. There have been a number of studies on flashback and their mechanisms leading to the following classification [12, 13]: (1) core flow flashback, (2) combustion instabilities, (3) vortex breakdown and (4) boundary layer flashback [14, 15]. The second and third mechanisms are not considered in this study. Core flow flashback occurs in freely propagating flames due to a kinematic imbalance between the turbulent flame speed and the local flow velocity [16, 17] and can be avoided by ensuring a sufficient kinematic balance in the burning zone [12, 16, 18]. By contrast, all premixed flames stabilised near walls are potentially susceptible to boundary layer flashback. This can be considered a special case of (1) where the flame propagates into regions of low velocity near the wall but has added complexity such as heat loss. Regardless, these different flashback mechanisms apply to systems operating in quasi-stationary regimes and it is not well understood what impact ignition has on flashback.

In a recent study [19], the ignition process was shown to induce a strong modulation in the injector mass flow in both a single sector and annular combustor. This is caused by volumetric expansion of burned gases resulting in a strong pressure perturbation which, in turn, modifies the air flowrate supplied to the burners leading to conditions favourable to flashback. It was observed that during the ignition transient, the flame switched from being anchored inside the injector to a lifted flame. It was later shown that the lower flame branch first flashes back before stabilisation is achieved [20].

The present work aims to improve our understanding of ignition generated flashback for hydrogen enriched flames. It is expected that for increasing hydrogen enrichment, the increased flame speed and diffusivity of hydrogen will increase the susceptibility of the system to flashback compared to premixed gaseous hydrocarbon flames such as methane. To do this, a series of ignition experiments using premixed methane-hydrogen blends with different levels of hydrogen enrichment were performed in a single sector combustor with varying back pressure. First, the impact of the back pressure on the ignition transient is presented and discussed. This is followed by a detailed analysis of two selected operating points to illustrate the effect of different levels of hydrogen enrichment. Finally, the effects of the fuel composition on the ignition dynamics are examined when keeping both the laminar burning velocity and bulk injector velocity constant for different levels of H_2-content.

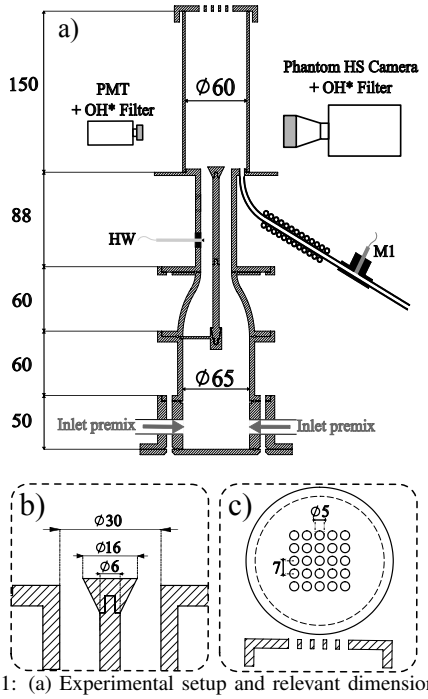

Fig. 1: (a) Experimental setup and relevant dimensions in millimeters. (b) Zoom of the burner outlet. (c) Combustion chamber exhaust with plate 25: $N \times N = 25$ holes.

2. Experimental setup and measurements

The experimental setup is presented in Fig 1a. Different blends of hydrogen, methane and air were premixed upstream and fed into the base of a cylindrical plenum which has a diameter $D_p = 65$ mm and a length $l_p = 90$ mm. The flow then passes through a converging section before entering a tube with an inner diameter $D = 30$ mm. Along the centre of the tube is a 6 mm diameter rod which is attached at the top of the plenum and holds a conical bluff body to stabilise the flame that has a diameter $D_b = 16$ mm as shown in Fig. 1b.

The flame is confined inside a cylindrical quartz combustion chamber of inner diameter $D_{cc} = 60$ mm. To impose different back pressures on the combustor, a set of perforated plates with varying porosity were used. Each plate had 5 mm holes uniformly distributed in a square pattern as shown in Fig. 1c. The number of holes was varied from $N \times N = 25$ to 16 to modify the porosity σ and vary the pressure drop ΔP at the combustor outlet as shown in Tab. 1. It is important to note that these small changes in the mean static pressure ΔP lead to significant changes in the over pressures generated during ignition.

The inlet velocity was measured 70 mm upstream of the bluff body using a hot wire probe (HW in Fig. 1a). The static and dynamic pressures were measured in the combustion chamber using a Kulite XCS-093-0.35D transducer placed in water-cooled wave guide, labelled M1 in Fig. 1a.

Table 1: Plate characteristics, plate porosity σ and pressure drop ΔP during cold-flow stationary conditions. The bulk velocity U_b is defined at the location of the hot wire probe.

	N × N	σ	ΔP	
			2 m.s^{-1}	5 m.s^{-1}
W/o Plate	-	1	~ 0 Pa	30 Pa
Plate 25	5×5	0.17	25 Pa	100 Pa
Plate 16	4×4	0.11	40 Pa	140 Pa

Flame images and time-series of OH* during ignition were measured using a Phantom V2012 high-speed camera with an intensifier (LaVision IRO) and a Hamamatsu H11902-13 photomultiplier (PMT) equipped with a UV filter centred at 310 ± 10 nm. Sampling rates of the PMT and high-speed camera were 52.5 and 10 kHz respectively. It is well established that OH* is a suitable proxy for the fluctuations in the heat release rate in premixed flames.

Care was taken to maintain constant thermal conditions during the ignition experiments. For each test the burner was preheated to a temperature $T_b = 470$ K measured at the center of the bluff-body using a pyrometer. The chamber was then filled with the combustible mixture for 5 s to ensure ignition occurred in a homogeneous mixture. A flame was then ignited using a spark plug positioned on the chamber back plate, approximately 20 mm away from the burner axis, located in the outer recirculation zone of the flow. The ignition system delivered spark energies of 36 mJ at $f = 50$ Hz. To avoid the saturation of the camera intensifier, a neutral density filter was used to mask the spark from the camera field of view.

The ignition dynamics were investigated for premixed H_2/CH_4-air mixtures with varying levels of H_2 enrichment characterized by the fraction of thermal power defined as $\mathrm{PH} = \mathcal{P}_{H_2}/(\mathcal{P}_{H_2} + \mathcal{P}_{CH_4})$. Ignition experiments were performed over a wide range of operating conditions from pure methane (PH0) to pure hydrogen (PH100) at different equivalence ratios ϕ for different pressure drops ΔP produced by perforated plates of different porosity placed at the top of the combustion chamber. The experiments were also performed for two bulk flow velocities $U_b = 2$ and 5 m/s at the injector exit under ambient temperature.

3. Stability maps

Stability maps showing the ignition limits for two bulk flow velocities U_b and three different back pressures are shown in Fig. 2. A minimum of five tests were done for each point. Three different ignition scenarios were observed:

- *Scenario A:* Soft ignition shown in green. Ignition leads to the formation of a flame kernel which propagates through the mixture and stabilises on the bluff-body.

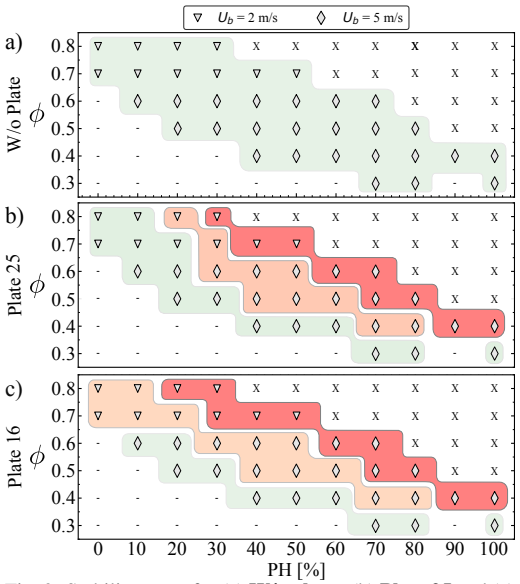

Fig. 2: Stability maps for (a) **W/o plate** , (b) **Plate 25** and (c) **Plate 16** configuration. The green shaded region represents the ignition *Scenario A*, the orange one *Scenario B* and the red one *Scenario C*.

- *Scenario B:* Temporary flashback shown in orange. Ignition immediately leads to flashback where the flame remains anchored upstream of the bluff body for a short time before it is advected downstream and stabilises on the bluff-body.
- *Scenario C:* Permanent flashback shown in red. Shortly after ignition flashback occurs and the flame remains stabilised upstream of the bluff body.

Videos of these different sequences are provided as supplemental material. The bottom left region in Fig. 2 with **-** symbols could not be explored due to the limits of the mass flow controllers. For CH_4-air flames, the point at $\phi = 0.6$ and $U_b = 5$ m.s^{-1} also corresponds to the lean blow off limit. The top right region with **X** symbols is limited by flashback which occurs at lower values of PH as ϕ increases. Note that when ϕ is constant, the thermal power $\mathcal{P}$, remains constant to within $\pm 5\%$ over all cases.

The green shaded region in Fig. 2a shows that atmospheric conditions promote a soft ignition process, *Scenario A*, for both U_b over all ϕ and PH. As there is no flow restriction at the exit of the combustion chamber, the combustion products can freely expand noting that the unsteady back pressure remains in this cases lower than $p_m \leq 0.5$ kPa during the ignition sequence as will be shown below.

The impact of increasing the back pressure is shown in Figs. 2b and 2c. Table 1 indicates that small increases in ΔP from 30 and 140 Pa at the combustor exit measured under stationary cold flow conditions has a strong effect on the ignition process. The

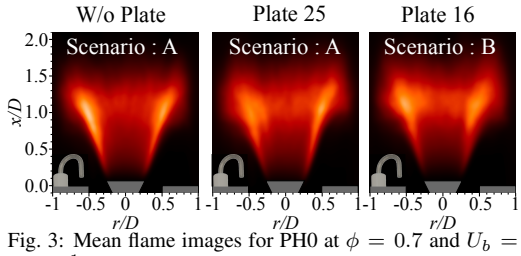

Fig. 3: Mean flame images for PH0 at $\phi = 0.7$ and $U_b = 2$ m.s^{-1} for three back pressures presented in Tab. 1.

green soft ignition region is considerably reduced as the exhaust pressure drop and hydrogen content increase in Figs. 2b-c. Temporary flashback *Scenarios B* and permanent flashback *Scenarios C* become more prevalent. Following a fixed value of ϕ, or iso-power, shows a clear transition from soft ignition to temporary flashback and then permanent flashback. Moreover, the increase in ΔP causes scenarios *B* and *C* to occur at progressively lower values of PH.

Despite the small values of Δp produced under steady cold flow conditions, they result in significant over pressures p_m during ignition causing strong flow modulations through the injector. The amplitude can vary from $p_m \simeq 2$ kPa for PH0 up to $p_m \simeq 5$ kPa for PH100 when $\Delta P = 100$ Pa and from 4 kPa to 8 kPa for PH100 when $\Delta P = 140$ Pa. This modifies the flow conditions promoting the flashback scenarios B and C. These effects are augmented by the higher reactivity of hydrogen leading to a higher acceleration of flame propagation after ignition which, in turn, generates a higher over pressure inside the chamber when the combustor back pressure is increased. This is further investigated in the next section by considering the transient response of the flame and the dynamic pressure.

4. Ignition dynamics

In the following, two specific flow conditions are considered: a CH_4-air flame (PH0) and CH_4/H_2-air flame (PH30) for the same operating conditions $U_b = 2$ m.s^{-1} and $\phi = 0.7$. Figure 2 shows that the PH30 flame switches from *Scenario A* to *B* and finally *C* when the mean back pressure is increased. The PH0 flame is taken as a reference to underline the impact of hydrogen.

4.1. PH0

Before discussing the ignition process and transient response, the effect of mean back pressure ΔP on the mean flame shape is considered. Figure 3 shows that the change in back pressure has a minimal effect as all flames show the expected V-flame structure. They feature similar lengths, flame angles and lift-off distances above the bluff body. Slight changes at the end of the flame brush are observed with an increase in ΔP. The different impedance of

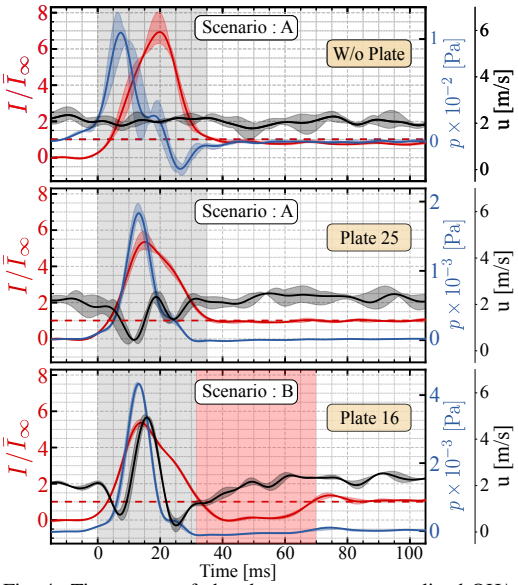

Fig. 4: Time traces of chamber pressure, normalized OH* light intensity and local flow velocity for PH0 at $\phi = 0.7$ and $U_b = 2$ m.s^{-1}. The time traces are averaged over 5 runs. The range of pressures varies in each plot.

the plates changes the acoustic reflection which modifies the combustion dynamics at the flame tip. This results in a small change in the mean heat release rate distributions near the top of the flame.

Time-resolved pressure, injector velocity, and OH* chemiluminescence were recorded simultaneously during the ignition process. Figure 4 plots their time-series averaged over five runs and corresponding signal "min-max" envelopes. The instant, $t = 0$ ms, marks the formation of the first flame kernel which rapidly grows as the fresh gases are quickly consumed leading to a steep increase in OH* reaching peak values between $t = 15 - 20$ ms. It quickly decays to the nominal value I_∞ which corresponds to the steady state of the flame. A similar trend in the dynamic pressure is observed but its time lag and amplitude relative to the OH* signal varies with ΔP. To ease interpretation of Fig. 4, the time-series data within the red and gray shaded regions correspond to flashback and ignition transient respectively. The transient ignition period remains roughly constant $\tau_p \sim 35$ ms in all three cases.

Without a perforated plate, the ignition process only generates a small over pressure $p_m \simeq 0.1$ kPa, which is not sufficient to modify the flow velocity inside the injector as shown by the black curve in Fig. 4. The addition of **Plate 25** and **Plate 16** increases the amplitude of p_m (blue curves) at ignition and generates correspondingly larger velocity oscillations inside the injector. For **Plate 25** the over pressure reaches $p_m \simeq 2$ kPa reducing the flow velocity through the injector to 0.6 m.s^{-1} at $t \approx 10$ ms. As p_m decays, the velocity continues to oscillate before

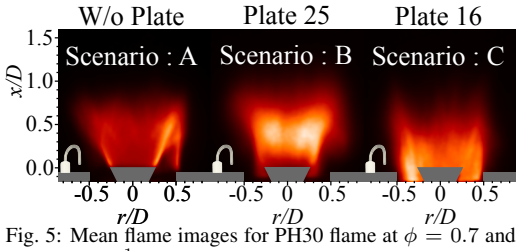

Fig. 5: Mean flame images for PH30 flame at $\phi = 0.7$ and $U_b = 2$ m.s^{-1}.

mean flow conditions are restored around $t = 30$ s. For **Plate 16** the over pressure reaches $p_m \simeq 4$ kPa in the bottom plot in Fig. 4 resulting in significant flow oscillations. As the pressure rises, the flowrate inside the injector first decreases but then rapidly accelerates as shown by the large overshoot which peaks around $u = 5.5$ m.s^{-1}, almost three times above U_b, before rapidly decelerating to $u \approx 0.1$ m.s^{-1}. This causes flashback to occur between $t = 30$ and $t = 70$ ms highlighted by the red shaded region before stabilising on the bluff body when $t > 70$ ms. This is shown by following the variation of the OH* signal over the same time period. Although the hot wire cannot detect reverse flow, it is 70 mm upstream, therefore as the velocity approaches zero indicates that reverse flow is likely to occur downstream of the measurement point. Another important feature is the time lag between the over pressure, velocity and OH* time-series between **Plate 25** and **Plate 16** which is discussed later in the paper.

4.2. PH30

A flame with the same U_b and ϕ but a higher hydrogen content, PH30, is now considered. Steady state flame images are shown in Fig. 5 for increasing ΔP. The electrode has been depicted in these pictures for context. It shows that the stability of the flame is very sensitive to the imposed back pressure. Without a plate, an M-shaped flame is stabilized on the bluff-body noting that the flame branch on the left side cannot be seen due to the use of a neutral density filter to avoid saturation of the intensifier during ignition. For **Plate 25**, flashback occurs and the flame is anchored upstream the bluff-body. In this case the flame exhibits large synchronized self-sustained oscillations leading to a higher OH* intensity in the wake region. **Plate 16** leads to permanent flashback as the flame remains stabilised inside the injector. It is worth noting that this behaviour was not observed when flames are ignited with only methane and the H_2-content is then slowly increased in a quasi-static way to reach the same enrichment.

The corresponding pressure and OH* times series are plotted in Fig. 6 supported by PIV data in the supplementary material. The hot wire probe could not be used due to flashback. Without any plate, the ignition dynamics leading to soft ignition scenario *A* is similar to that observed in Fig. 4 for the PH0 case.

The main differences are that the ignition transient (grey shaded region) is slightly shorter $\tau_p \sim 25$ ms and p_m is approximately twice the value compared with the PH0 case. For **Plate 25**, the over pressure peak reaches $p_m \sim 4$ kPa which is of the same order of magnitude as for PH0 with **Plate 16** in Fig. 4. In both cases, this leads to *Scenario B* due to the decrease in the injector velocity which is proportional to $1/p_m$ (See the supplementary materials for more details). For **Plate 16**, the over pressure further increases to $p_m \sim 5.5$ kPa resulting in permanent flashback of the flame, i.e. *Scenario C*. It also leads to large pressure oscillations beyond $t > 20$ ms due to large oscillations of the flame as it cannot properly anchor in the plenum. These changes in the ignition dynamics with H_2-enrichment are the consequence of the higher laminar burning velocity which is roughly increased by a factor of 2 from $S_l^0 = 0.19$ m.s^{-1} for PH0 to $S_l^0 = 0.35$ m.s^{-1} for PH30 resulting in larger flow accelerations at the exit of the injector as the flame kernel develops [19].

The results for PH0 and PH30 show that the main mechanism driving flashback is the transient, high amplitude over pressures. The over pressure amplitude is very sensitive to the mean combustor back pressure as shown by the addition of the porous plates. During the ignition transient, the flame acts as a piston moving at the absolute flame speed $S_a = \mathbf{w} \cdot \mathbf{n}$ [21] which pushes away fresh gases [20]. The addition of porous plates lead to small increases of the mean back pressure amplifying the amplitude of pressure perturbations due to ignition, which in turn modify the flow response through the injector promoting flashback. However, the results also suggest that the synchronization of the pressure and OH* signals also plays an important role in triggering flashback. This makes it difficult to isolate the role of over pressure and H_2-content on flashback.

5. Impact of hydrogen enrichment

An attempt is made to isolate effects of combustion properties of hydrogen from the flow dynamics by keeping both the bulk velocity and the laminar burning velocity fixed at $U_b = 5$ m.s^{-1} and $S_l^0 = 0.25$ m.s^{-1} respectively for increasing levels of hydrogen enrichment. To maintain a fixed burning velocity S_l^0, ϕ was varied in accordance with Tab. 2. Keeping U_b and S_l^0 constant necessarily results in a change in the thermal power.

Figure 7 shows average time-series of dynamic pressure measured in the combustor and OH* emission during ignition for different levels of H_2-enrichment (PH%). Averages were obtained for a minimum of 5 runs for each PH. For brevity, the results are only presented for case **Plate 25**. Figure 7a shows that keeping U_b and S_l^0 constant effectively scales the response of the pressure time-series. All levels of PH achieve approximately the same over pressure $p_m \simeq 5$ kPa, which consequently leads to a similar flow perturbation within the injector. This

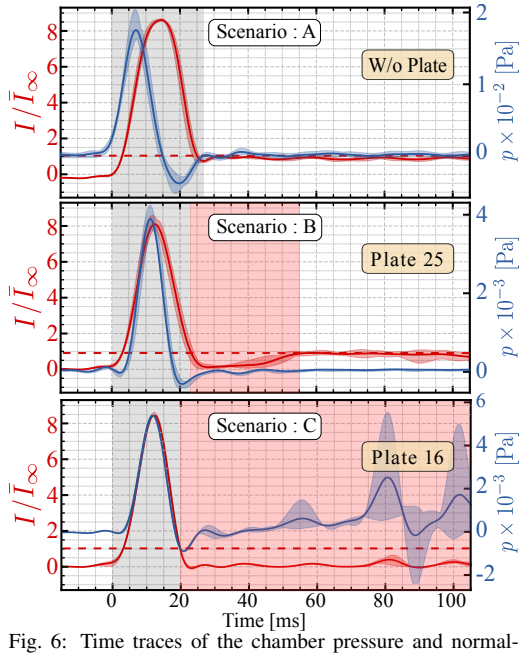

Fig. 6: Time traces of the chamber pressure and normalized light intensity averaged for PH30 flame at $\phi = 0.7$ and $U_b = 2$ m.s^{-1}. Solid lines stand for the average signal over the runs. The envelope of all runs is also plotted.

result confirms that for a constant laminar burning velocity S_l^0, the effects of thermal expansion and flame propagation during ignition remain comparable and are independent of the level of H_2-enrichment.

Although good collapse of the over pressures with S_l^0 is found, Fig. 7b shows that the flame stabilization process differs with PH. From PH0-PH20 soft ignition and stabilization processes occur with *Scenario A*. At PH40, temporary flashback occurs with *Scenario B* between 15 ms $\leq t \leq$ 40 ms before stabilizing at the bluff body. Once $\mathcal{P}_{H_2} > 40\%$ all the flames permanently flashback with *Scenario C* immediately after ignition. This shows that flashback cannot be a function of S_l^0 only and that the level of H_2-enrichment needs also to be considered.

The effect of H_2-enrichment on the flame response cannot be fully explained using classical kinematic arguments which suggest that flashback is mainly driven by an imbalance in the kinematic equilibrium

Table 2: Operating conditions for different levels of H_2-enrichment keeping both the bulk velocity $U_b = 5$ m.s^{-1} and the laminar burning velocity $S_l^0 = 0.25$ m.s^{-1} fixed.

Cases	ϕ	$\mathcal{P}_{CH_4}$	$\mathcal{P}_{H_2}$	$\mathcal{P}$ [kW]
PH0	0.78	100%	0%	8.4
PH20	0.68	80%	20%	7.6
PH40	0.60	60%	40%	6.9
PH60	0.53	40%	60%	6.3
PH80	0.48	20%	80%	6.0
PH100	0.43	0%	100%	5.7

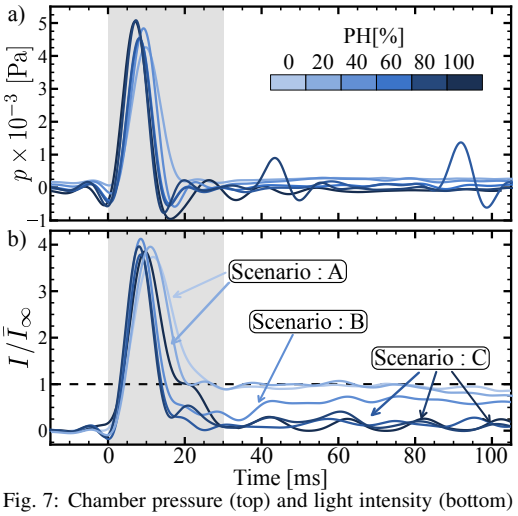

Fig. 7: Chamber pressure (top) and light intensity (bottom) signals for the six flames presented in Tab. 2 with Plate 25.

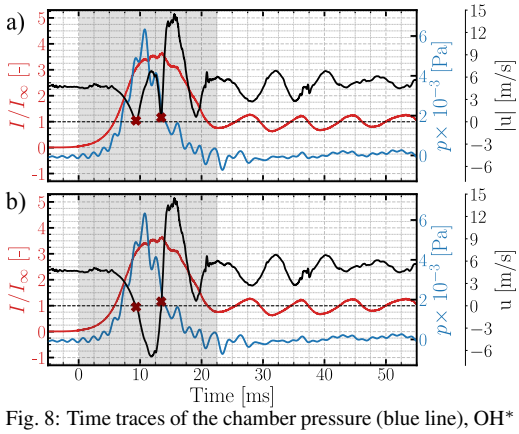

Fig. 8: Time traces of the chamber pressure (blue line), OH* light intensity (red line) and injector flow velocity (black line) for a single run for PH0 flame in Tab. 2. a) shows the absolute injector flow velocity measured by the hot wire and b) denotes the real velocity signal.

between the local flow and burning velocities. For example, simple flashback criteria are often defined when the ratio (U_b/S_l^0) drops below a critical threshold value $(U_b/S_l^0)_c$ [13, 16]. In these experiments, the ratio (U_b/S_l^0) is kept constant, yet the susceptibility to flashback increases with increasing hydrogen enrichment. Furthermore, since the over pressure remains also the same in all cases, the increased propensity for flashback cannot be due to differences in the injector flow dynamics. Preferential diffusion effects must therefore play a crucial role. One also needs to keep in mind that the unsteady flame front is highly wrinkled and propagates anisotropically. These local effects cannot be captured using the photomultiplier (PMT in Fig. 1).

Two conditions need to be simultaneously met to allow the flame to propagate into the injector. First, the ratio (U_b/S_l^0) needs to drop below the critical flashback limit $(U_b/S_l^0)_c$, second, the flame must be within the vicinity of the injector. Synchronisation of these two events is therefore essential. The first condition is set by the amplitude of the over pressure and the critical threshold $(U_b/S_l^0)_c$ which is kept constant. The critical threshold is expected to be lower for H_2-enriched flames given that S_l^0 is lower than the real flame displacement speed S_d. For lean hydrogen mixtures, S_d exceeds S_l^0 due to the imbalance between heat and species diffusion in flames characterized by non-unity Lewis numbers which generates reaction layer instabilities [22].

In the cases explored during this study, pressure peaks larger than $p_m \simeq 4$ kPa led to a temporary reverse flow inside the annular injector as highlighted in Fig. 8.a. This figure plots the non-filtered time series of a single run for PH0 flame in Tab. 2. It clearly shows that the pressure perturbation leads to a temporary reverse flow between $t = 8$ ms and $t = 13$ ms as the velocity signal measured by a hot wire (HW in Fig. 1) first drops to zero at $t = 8$ ms, then rapidly increases before dropping down again to zero at $t = 13$ ms followed by a large overshoot reaching a peak around $u \simeq 14$ m.s^{-1}. Since the hot wire measures only the the absolute component of the velocity, the real velocity signal is reconstructed and plotted in Fig. 8.b with negative velocities between 8 ms $\leq t \leq$ 13 ms that drops down to $u \simeq -6$ m.s^{-1} at $t \simeq 11.6$ ms. This instant approximately matches the instant $t = 11.2$ ms when the pressure reaches its maximum. This observation indicates that the first condition for flashback is always satisfied in Fig. 7 regardless of the H_2-content in the fuel. Despite the strong reverse flow, the flame smoothly ignites following ignition *Scenario A* in Fig. 8 demonstrating that the first condition based on the kinematic balance between the reactant flow velocity and burning velocity is a necessary but not sufficient condition to trigger flashback.

The second condition considers the location of flame propagation and advection in the volume and cannot be verified via PMT data. Nevertheless, the synchronization of these two events can be investigated by evaluating the time-lag τ between the peak over pressure and OH* time-series as shown in Fig. 9. It was previously shown that the instant corresponding to the peak p_m also coincides with the minimum velocity inside the injector (see Fig. 8). If the OH* peak is considered to mark the instant when all the fresh gases have been consumed and therefore, corresponds to the time when the flame is stabilized on the bluff-body, then, as τ tends to zero, the time synchronisation condition is satisfied increasing the risk of flashback. In particular, if the velocity inside the injector is sufficiently low, both conditions are met and the lower flame branch can propagate upstream into the injector causing flashback. On the other hand, when τ is large enough, the sudden velocity drop inside the injector occurs before the flame has time to

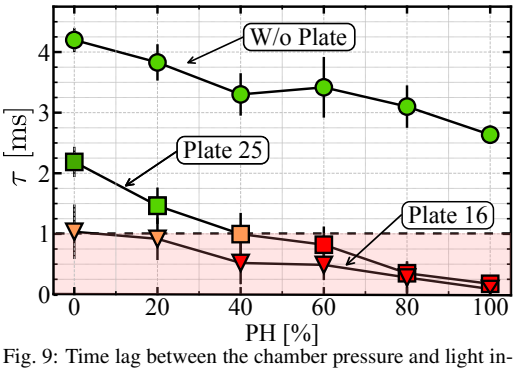

Fig. 9: Time lag between the chamber pressure and light intensity peaks for the three configurations presented in Tab. 1. Green symbols: ignition *Scenario A*. Orange symbols: *Scenario B*. Red symbols: *Scenario C*. The black dashed line corresponds to $\tau_c = 1$ ms.

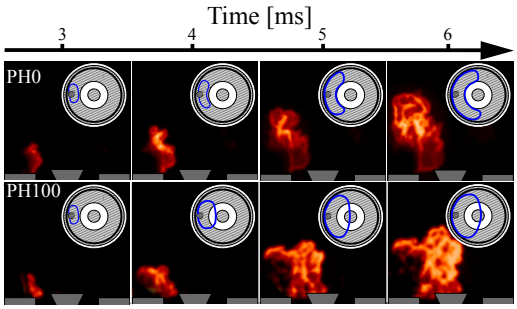

Fig. 10: Instantaneous OH* snapshots highlighting flame propagation after ignition for $S_l^0 = 0.25$ m.s^{-1} and $U_b = 5$ m.s^{-1}. Top row: PH0. Bottom: PH100. Operating conditions are given in Tab. 2. On the top right of each image, a sketch of the overhead view is drawn to delineate the flame position represented in blue.

reach the injector orifice and flashback is avoided.

Based on the data, a critical value $\tau_c \sim 1$ ms is identified as the minimum time lag $\tau > \tau_c$ above which the synchronisation condition is not satisfied and the ignition leads to *Scenario A* (green symbols in Fig. 9). Conversely, when $\tau < \tau_c$, the flame flashes back and leads to *Scenario C* shown by the red symbols. When $\tau \sim \tau_c$, the ignition develops *Scenario B* (orange markers) characterized by transient flashback. Figure 9 also shows that the delay τ decreases with increasing ΔP. This decay is partly related to the inertial time τ_f needed to displace the column of fluid by thermal expansion of the burned gases which can be considered as the sum of two time scales $\tau_f = \tau_l + \tau_\delta$. The first delay $\tau_l = l_c/S_a$ denotes the time required for the flame propagating at absolute speed S_a to cross the length l_c of the combustion chamber. The additional delay $\tau_\delta = \delta\sigma/S_a$ is due to the inertia of the fluid exhausting through the holes of the perforated plate, where δ is the sum of the plate thickness and an end correction which depends only on the diameter of the holes and σ is the plate porosity. In the conditions explored, τ_l is fixed and since τ_δ is proportional to σ, τ_f decreases with increasing ΔP.

For a fixed porosity, τ also reduces in Fig. 9 with hydrogen enrichment. This might be linked to the drop of the ignition time delay τ_i, defined here as the time interval between the first spark and the sudden rise of OH* emission. With this definition, experiments show that τ_i decreases from $\tau_i \sim 5$ ms for PH0 to $\tau_i \sim 0.2$ ms for PH100. However, this gap does not correspond to those observed in Fig. 9 when one switches from PH0 to PH100 for a given back pressure. A drop in τ_i also implies an increase in the flame speed. This would lead to an increase in over pressure as shown in Section 4, which is not observed here.

Resistance to stretch can also affect flame propagation during ignition. Pouech et al. [8] showed that the development of a flame kernel initiated in a recirculation zone can be quenched when entering in a high-shear region of the flow where the local strain rate exceeds the critical extinction strain rate. In these experiments, the shear and strain rates produced by the annular jet in cold flow conditions are the same for all combustible mixtures. Due to their higher resistance to strain, flames with higher levels of H_2-enrichment can propagate into regions of more intense shear and propagate through the annular jet shear layer.

This interpretation is qualitatively supported by Fig. 10 which shows instantaneous OH* images between $t = 3$ ms and $t = 6$ ms after ignition. For the PH0 flame at the top in Fig. 10, the heat release rate distribution is not uniform along the flame front. The upper flame branch is distinguished by a high intensity and the lower flame branch, slightly lifted, with a lower light intensity. The overhead views show that the flame cannot cross the jet shear layer and stabilises along the shear layer by propagating around it. The PH100 flame at the bottom in Fig. 10 shows a homogeneous heat release rate distribution along the flame front with a lower flame branch that is already propagating in the upstream direction through the injector for $t \geq 5$ ms. The overhead view shows the flame propagating through the jet shear layer towards the bluff-body which results in flashback when the flow rate drops. Finally, for lean hydrogen enriched flames thermo-diffusive effects can counteract the effects of strain enabling flame propagation through regions of high shear due the effects of preferential diffusion which leads to local enrichment along the reaction front and a higher local burning velocity [22].

6. Conclusion

The impact of chamber back pressure and increasing H_2-enrichment on the ignition dynamics of premixed bluff body flames has been investigated. It has been shown that the propensity of the flame to flashback depends on both the amplitude of the over pressure produced by ignition and the level of H_2-enrichment. Using perforated plates of different

porosity to vary the back pressure, it was shown that small changes in the pressure drop amplify the pressure perturbations at ignition leading to very large over pressure amplitudes and promoting flashback. The large amplitude over pressures reduce the reactant flowrate at the injector exit facilitating flame propagation in the upstream direction.

The amplitude of the over pressure was shown to scale with the ratio of bulk velocity to laminar burning velocity. However, for a fixed over pressure the risk of flashback was found to increase with increasing levels of H_2-enrichment. Two mechanisms were considered to explain this behavior, including a shift of the quasi-static flashback limit due to an increase of the flame speed and an increased resistance to stretch with a higher extinction limit of the propagating reaction layer. The latter effect is due to the high diffusion rate of hydrogen which enables flames to propagate through regions of high shear whereas mixtures with little or no hydrogen are extinguished.

For a given over pressure, the risk of flashback increases when the peak of the over pressure coincides with the peak of heat release rate. This synchronization is necessary to get a flame front close to the burner outlet when the flow velocity drops inside the burner. When the time lag between the peak pressure and heat release rate increases, the risk of flashback is substantially reduced.

Acknowledgments

The authors acknowledge support from the NCCS Centre, funded under the Norwegian research program, Centres for Environment-friendly Energy Research (FME) (Grant 257579/E20).

Supplementary material

Videos of the three different scenarios, effect of the chamber length on the ignition dynamic as well as instantaneous PIV snapshots for PH30 flame at $U_b = 2$ m.s^{-1} and $\phi = 0.7$ are provided as supplementary material.

References

[1] S. Taamallah, K. Vogiatzaki, F. M. Alzahrani, E. M. Mokheimer, M. Habib, A. F. Ghoniem, Fuel flexibility, stability and emissions in premixed hydrogen-rich gas turbine combustion: Technology, fundamentals, and numerical simulations, Appl. Energy 154 (2015) 1020–1047.

[2] A. L. Sánchez, F. A. Williams, Recent advances in understanding of flammability characteristics of hydrogen, Prog. Energy Combust. Sci. 41 (2014) 1–55.

[3] D. Ballal, A. Lefebvre, Ignition and flame quenching in flowing gaseous mixtures, Proc. R. Soc 357 (1689) (1977) 163–181.

[4] E. Mastorakos, Forced ignition of turbulent spray flames, Proc. Combust. Inst. 36 (2) (2017) 2367–2383.

[5] J.-F. Bourgouin, D. Durox, T. Schuller, J. Beaunier, S. Candel, Ignition dynamics of an annular combustor equipped with multiple swirling injectors, Combust. Flame 160 (8) (2013) 1398–1413.

[6] E. Machover, E. Mastorakos, Experimental investigation on spark ignition of annular premixed combustors, Combust. Flame 178 (2017) 148–157.

[7] T. Marchione, S. F. Ahmed, E. Mastorakos, Ignition of turbulent swirling n-heptane spray flames using single and multiple sparks, Combust. Flame. 156 (1) (2009) 166–180.

[8] P. Pouech, F. Duchaine, T. Poinsot, Premixed flame ignition in high-speed flows over a backward facing step, Combust. Flame. 229 (2021) 111398.

[9] F. Halter, C. Chauveau, N. Djebaïli-Chaumeix, I. Gökalp, Characterization of the effects of pressure and hydrogen concentration on laminar burning velocities of methane–hydrogen–air mixtures, Proc. Combust. Inst. 30 (1) (2005) 201–208.

[10] C. Liew, H. Li, J. Nuszkowski, S. Liu, T. Gatts, R. Atkinson, N. Clark, An experimental investigation of the combustion process of a heavy-duty diesel engine enriched with h2, Int. J. Hydrog. Energy. 35 (20) (2010) 11357–11365.

[11] M. Weinrotter, H. Kopecek, M. Tesch, E. Wintner, M. Lackner, F. Winter, Laser ignition of ultra-lean methane/hydrogen/air mixtures at high temperature and pressure, Exp. Therm. Fluid Sci. 29 (5) (2005) 569–577.

[12] T. Lieuwen, V. McDonell, D. Santavicca, T. Sattelmayer, Burner development and operability issues associated with steady flowing syngas fired combustors, Combust. Sci. Technol. 180 (6) (2008) 1169–1192.

[13] A. Kalantari, V. McDonell, Boundary layer flashback of non-swirling premixed flames: Mechanisms, fundamental research, and recent advances, Prog. Energy Combust. Sci. 61 (2017) 249–292.

[14] A. Gruber, J. H. Chen, D. Valiev, C. K. Law, Direct numerical simulation of premixed flame boundary layer flashback in turbulent channel flow, J. Fluid Mech. 709 (2012) 516–542.

[15] D. Ebi, N. T. Clemens, Experimental investigation of upstream flame propagation during boundary layer flashback of swirl flames, Combust. Flame 168 (2016) 39–52.

[16] A. C. Benim, K. J. Syed, Flashback mechanisms in lean premixed gas turbine combustion, Academic press, 2014.

[17] B. Lewis, G. von Elbe, Stability and structure of burner flames, J. Chem. Phys 11 (2) (1943) 75–97.

[18] J. F. Driscoll, Turbulent premixed combustion: Flamelet structure and its effect on turbulent burning velocities, Prog. Energy Combust. Sci. 34 (1) (2008) 91–134.

[19] K. Prieur, G. Vignat, D. Durox, T. Schuller, S. Candel, Flame and spray dynamics during the light-round process in an annular system equipped with multiple swirl spray injectors, J. Eng. Gas Turb. Pow. 141 (6) (2019).

[20] K. Töpperwien, F. Collin-Bastiani, E. Riber, B. Cuenot, G. Vignat, K. Prieur, D. Durox, S. Candel, R. Vicquelin, Large-eddy simulation of flame dynamics during the ignition of a swirling injector unit and comparison with experiments, J. Eng. Gas Turb. Pow. 143 (2) (2021) 021015.

[21] T. Poinsot, D. Veynante, Theoretical and numerical combustion, RT Edwards, Inc., 2005.

[22] L. Berger, A. Attili, H. Pitsch, Intrinsic instabilities in premixed hydrogen flames: parametric variation of pressure, equivalence ratio, and temperature. part 2–non-linear regime and flame speed enhancement, Combust. Flame. 240 (2022) 111936.